JOURNAL OF APPLIED ELECTROCHEMISTRY **28** (1998) 1351–1357

Electrochemical behaviour of iron and copper in a culture solution for *Spirulina platensis*

R. MALGOR, G. HEIJO, L. ROMERO, C. F. ZINOLA*

Electrochemistry and Corrosion Department, School of Science and Engineering, Libertad Str., 2497, C.P. 11300, Montevideo, Uruguay

Received 11 April 1997; accepted in revised form 26 May 1998

Cyclic voltammograms of iron and copper electrodes were run in sodium hydroxide, carbonate–bicarbonate buffer and culture media for *Spirulina platensis* at 30 °C. Potentiostatic steady state polarisation curves for both electrode surfaces in these electrolytes were performed in the presence and the absence of *S. platensis* at fixed temperature. Corrosion potential and corrosion current density values of iron and copper were obtained graphically from these curves. In all cases, the largest corrosion current density corresponded to the maximum biogenerated-oxygen concentrations, that is, illuminated culture media containing *S. platensis*. Corrosion potentials of iron electrodes shifted to positive values for increasing corrosion rates, whereas constant corrosion potentials were obtained for copper electrodes independently of the electrolyte.

Keywords: *copper*, *corrosion*, *cyclic voltammetry*, *iron*, *Spirulina platensis*

1. Introduction

Spirulina platensis is a cyanophyte microalgae, that grows in natural or alkaline mineralized waters at temperatures higher than 30 °C [1–3]. The presence of the microalgae in solution increases the oxygen partial pressure at the interface as a consequence of the oxygen biogeneration, particularly after a long exposure to light [4]. Thus, oxygen biogeneration can produce a threefold increase in the solution oxygen level *vis á vis* that expected from atmospheric equilibrium [5]. Cultivation of *S. platensis* requires temperatures higher than 30 °C (optimum growth) [6], which are generally achieved in baths thermally stabilised by copper or iron calefactors in direct contact with the culture solution. The presence of microorganisms and their metabolic products may induce the metal corrosion. Moreover, the kinetics of the microbial corrosion is affected by changes in temperature and in the solution composition (metabolic products and oxidising agents) [7, 8].

These facts encouraged us to study the electrochemical behaviour of iron and copper in alkaline and bioactive microalgae-containing solutions, using cyclic voltammograms, polarization curves and the time evolution of the rest potentials. From electrochemical kinetic data, corrosion potentials and corrosion current densities were determined.

2. Experimental details

Cyclic voltammograms were run with iron (99.8% purity) and copper (99.98% purity) wire electrodes of 1 mm diameter, and with commercially available metal plates (~5 cm^2); that is, iron (96% purity) containing nickel (1.5%), chromium (1.4%), copper (0.3%), molybdenum (0.1%), carbon (0.6%) and silicon (0.2%); and copper (95% purity) plates containing nickel (1.9%), aluminium (1.2%), zinc (0.5%), magnesium (0.2%) and tin (0.4%). Polarization curves were performed with both high-purity and commercially pure metal probes. In both cases, the electrochemical system was completed with a platinum plate (10 cm^2 geometric area) counter electrode and a silver/silver chloride (4 M potassium chloride) reference electrode. All potentials in the text are referred to the normal hydrogen electrode (NHE).

The working solutions, 0.1 M NaOH, carbonate–bicarbonate buffer (pH 9.9) and culture medium (SOT), were prepared from Millipore-MilliQ* water and analytical grade chemicals. One litre of the culture medium contains: 16.8 g $NaHCO_3$, 0.5 g K_2HPO_4, 2.5 g $NaNO_3$, 1.0 g K_2SO_4, 1.0 g NaCl, 0.2 g $MgSO_4.7\,H_2O$, 0.04 g $CaCl_2.2\,H_2O$, 0.01 g $FeSO_4.7\,H_2O$, 0.08 g EDTA and 1.0 ml of a micronutrient-containing solution (A). One litre of solution A contains: 2.86 g H_3BO_3, 1.81 g $MnCl_2.4\,H_2O$, 0.22 g $ZnSO_4.7\,H_2O$, 0.04 g $NaMoO_4.2\,H_2O$, 0.08 g $CuSO_4.5\,H_2O$, 0.05 g $Co(NO_3)_2.6\,H_2O$. The pH of a freshly prepared SOT solution is 9.7.

The electrochemical runs were performed with a LYP M7 potentiostat–galvanostat, a LYP WT function generator and an X–Y–*t* Linseis recorder.

2.1. *Cyclic voltammograms*

Voltammetric experiments were performed in a conventional electrochemical cell with the reference

* To whom correspondence should be addressed.

electrode shielded in a double glass frit compartment. The working solutions were oxygen-free 0.1 M NaOH, carbonate–bicarbonate buffer and SOT without *S. platensis*. Nitrogen (99.99% pure) was bubbled through the solution to remove oxygen.

2.1.1. Working electrode pretreatments. Cyclic voltammograms were obtained with copper and iron electrodes in oxygen-free 0.1 M NaOH, carbonate–bicarbonate buffer and SOT without *S. platensis* at a sweep rate of 0.05 V s^{-1} and 30 °C. Reproducible results and well-defined peaks in the voltammetric contours were obtained, when the surfaces were treated as follows [9]. Iron electrode: (i) cleaning with ketone, (ii) washing with Millipore-MilliQ* water and (iii) dipping in 6 M HCl for 30 s. Copper electrode: as steps (i) and (ii) above then, finally, dipping in 10% H_2SO_4 for 3 s.

After the metal pretreatment, and before each cyclic voltammetric run, the electrode surfaces were activated by applying a square wave potential routine, comprising a first 0.5 V step during 5 s, to remove the surface microimpurities, and a further −1.2 V step for 2 min to electroreduce the metal surface. This potential program allowed all the voltammetric runs to be started with a completely activated and reduced surface [10].

2.2. *Polarization curves*

Potentiostatic steady state polarization curves, plotted as potential against log(current density) profiles, were performed in 0.1 M NaOH and SOT (with and without *S. platensis*) at 30 °C. Nitrogen, oxygen (99.9% purity) and dry air were bubbled through the electrolytes until saturation to perform the electrochemical kinetic experiments. Prior to each run, the metal surfaces were chemically treated to remove the corrosion products from the metal as mentioned above [9].

Two equivalent metal probes were used to perform, independently, the anodic and cathodic branches of the polarization curves. However, the open-circuit potential of the system, E_{rest}, was measured previously to be sure that the surface was polarized from the same initial potential. Polarization curves were performed on both electrodes by applying potential steps of 5 to 10 mV starting from E_{rest} and polarizing the metal in the anodic or cathodic directions within the −1.5 to 1.2 V potential range. The steady state current densities were recorded after each potential step either in alkaline or in culture media (with and without *S. platensis*), at 30 °C. The corrosion potential, E_{corr}, and the corrosion current density, j_{corr}, of each system, were calculated graphically from the potential against log(current density) plots.

2.3. *Spirulina platensis cultivation and characterization*

S. platensis was cultivated in a cylindrical transparent glass reactor of 1.5 litre capacity, agitated with air at a pressure of 2.5 psi with a flux of 0.7 l min^{-1}. The photoperiod of the culture medium was; illuminated for 4 h at 5.4 klux and 2 h in the dark, both at 30 °C. The growth of bacteria and dinoflagellate species was inhibited in the culture medium by adding oxytetracycline (antibiotic) and ammonium chloride, respectively [1]. Figure 1 shows the microalgae growth curve, plotted as absorbance at 560 nm against time. The spectrophotometric data were obtained using a Spectronic 20. Figure 2 shows the plot of the oxygen concentration against light-phase period. Zero time in the light phase was considered as the beginning of the illuminated period. The oxygen concentration was followed with an YSI 57 model oxygen sensor. Both curves characterize the microalgae growth as a function of time. The culture solutions used in the performance of the electrochemical kinetic runs were chosen as the basis of these curves. Thus, culture media C_1 and C_2 were the solutions at the 5th and 20th day of the growing phase, respectively, characterized by data presented in Table 1. In this respect, C_1 was the medium in which the slope of the oxygen concentration against light-phase period curve was optimum (high oxygen levels), whereas C_2 corre-

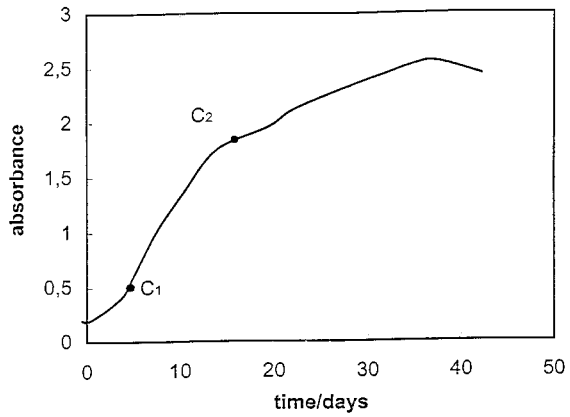

Fig. 1. Absorbance at 560 nm against time (days) plot. C_1 and C_2 are the culture media at the 5th and 20th day, respectively.

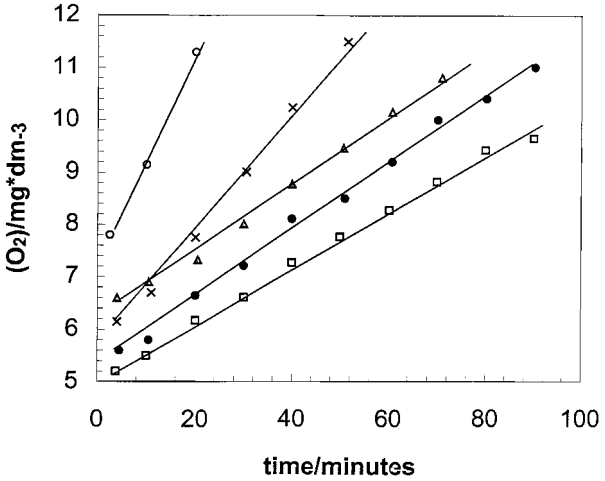

Fig. 2. Dissolved oxygen concentration (mg dm^{-3}) dependence on the light-phase time (minutes). Plots (△), (●) and (×) are three consecutive days from zero time. Plots (○) and (□) are the corresponding curves at 5th and 20th days, respectively.

Table 1. Spirulina platensis harvest time parameters characterized by oxygen concentrations (ppm), absorbance at 560 nm and pH

	C_1	C_2
Oxygen concentration	9.1	5.8
Absorbance	0.45	1.65
pH	9.9	10.0

sponded to the smallest slope of that curve (low oxygen levels). The large oxygen concentrations reached in the microalgae culture medium produce an increase in the cellular reproduction rate. However, there are two counter effects involved in the evolution of the culture medium, that is, large cellular concentrations increase the oxygen biogeneration, but reduce the light incidence in solution. Both facts lead to a lower photosynthetic activity.

3. Results and discussion

3.1. *Cyclic voltammetric experiments*

3.1.1. Cyclic voltammograms of iron electrodes. Figure 3 shows the cyclic voltammogram of a high-purity iron electrode run at $0.05\,V\,s^{-1}$ in deoxygenated aqueous 0.1 M NaOH and SOT free of *S. platensis* at 30 °C. The cyclic voltammetric profiles of iron in NaOH define four anodic peaks that result from the progressive iron electrooxidation. The cyclic voltammogram run of a commercially pure electrode lacks definition and quality and is not presented here; however, the type and number of voltammetric peaks are the same.

The anodic scan leads to a current plateau at potentials higher than 0.4 V, typical of a passive layer. The composition of the iron oxides and the passive layer depends on the nature of the electrolyte and temperature [11]. All peak currents increase linearly with the potential sweep rate. Nevertheless, potential sweeps greater than $0.10\,V\,s^{-1}$ produce a larger increase in the current and peak IV charge than on the other anodic peaks (Table 2).

Table 2. Iron voltammetric current peaks (mA) as a function of the potential sweep rate ($V\,s^{-1}$) in aqueous 0.1 M NaOH at 30 °C

Sweep rate	*Peak I*	*Peak II*	*Peak III*	*Peak IV*	*Peak V*	*Peak VI*
0.01	0.12	0.08	0.23	0.11	1.74	1.24
0.02	0.23	0.19	0.45	0.23	3.23	2.43
0.05	0.59	0.42	1.02	0.57	6.07	5.86
0.10	1.02	0.87	2.19	1.34	12.63	10.55
0.15	1.57	1.25	3.27	2.67	17.81	14.98
0.20	2.08	1.71	4.24	3.78	23.58	21.55
0.25	2.64	2.03	5.36	4.99	27.82	26.72
0.30	3.19	2.54	6.34	6.89	37.46	32.46

The potentiodynamic behaviour of iron electrodes in the deoxygenated electrolytes (without *S. platensis*), showed two electroreduction peaks and a total oxide reduction process taking place at peak VI. Peak I is not considered in the analysis of the iron oxide electroformation, since it is the result of a combined process, that is, the early stages of iron electrodissolution process and the H-atom electrodesorption reaction [12]. The four anodic contributions observed for iron in NaOH are displayed as humps or broad asymmetric peaks in SOT. Moreover, the lower potential limit of the cathodic sweep can be extended towards more negative values in SOT. This is the consequence of the adsorption of diverse anions on iron and the inhibition of the H-atom electroadsorption process.

As a control experiment, the cyclic voltammogram of a high-purity iron was run in a buffered solution (pH 9.9) at $0.05\,V\,s^{-1}$ (Fig. 4). Almost the same trends as in SOT are observed, but with a greater definition of the voltammetric peaks and the appearance of a new electroreduction peak (denoted as V′) at about 0 V. The anodic voltammetric peak shows almost the same trends as in the culture solution. It should be noted that the cyclic voltammogram performed for a commercially pure iron, exhibited poor quality but the same potentiodynamic contour.

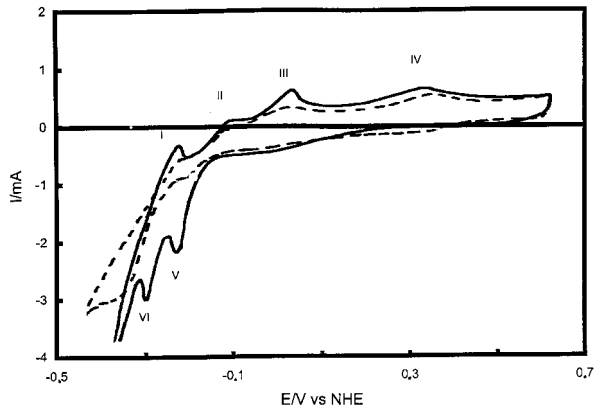

Fig. 3. Cyclic voltammogram of high-purity iron in aqueous 0.1 M NaOH (—) and SOT medium (- - -) run at $0.05\,V\,s^{-1}$ and 30 °C.

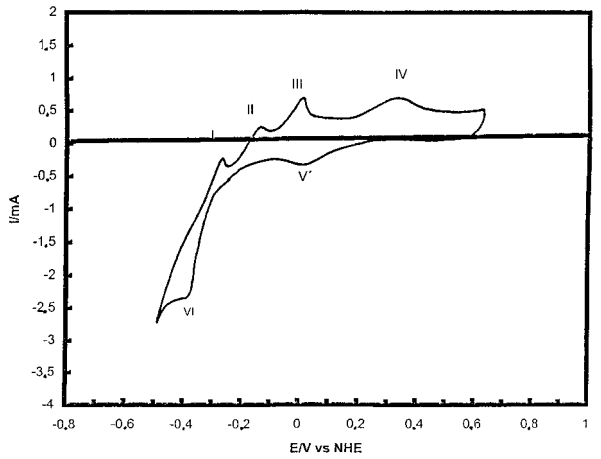

Fig. 4. Cyclic voltammogram of high-purity iron in deoxygenated carbonate–bicarbonate buffer solution run at $0.05\,V\,s^{-1}$ and 30 °C.

3.1.2. Cyclic voltammograms of copper electrodes. The potentiodynamic current/potential profiles of copper electrodes in deoxygenated 0.1 M NaOH and SOT free of *S. platensis* are presented as superimposed curves in Fig. 5.

The cyclic voltammograms exhibit complex anodic and cathodic contours in both NaOH and SOT; however, better definition and sharpness were obtained in NaOH. Voltammetric peak I in NaOH is the result of the initial OH-electroadsorption process on copper, whereas peak II (0.46 V) and III (0.80 V) represent the electroformation of massive Cu(I) and Cu(II) oxides [10, 11]. The electroreduction of these two oxides is accomplished in the cathodic sweep at 0.60 V (peak IV) and 0.28 V (peak V), that is, corresponding to the phase changes of the former oxides (peak III and peak II, respectively). For potentials lower than 0.1 V, two cathodic peaks, at about 0.04 V (peak VI) and at −0.19 V (peak VII) develop before the hydrogen evolution reaction. There is still doubt about the nature of the species responsible for these peaks, however VI has been explained as the voltammetric result of passivated copper oxide electroreduction, and VII as a H-atom electroadsorption process on a well-reduced copper surface [11].

Cyclic voltammetric results of copper in oxygen-free SOT are different from those in NaOH. Anodic voltammetric peaks II* and III* in SOT exhibit a narrower potential window than the II and III analogue-peaks in alkaline solutions. The copper-oxide electroreduction peaks (IV* and V*) also behave in the same way as the anodic conjugated couples. This is probably the result of the lower OH^- ion concentration in SOT which gives a narrower potential window, and the higher ionic force of SOT which leads to a lower copper oxide onset potential.

The cyclic voltammogram for high-purity copper in carbonate–bicarbonate buffered solution at $0.05\,V\,s^{-1}$ was also determined (Fig. 6). The voltammetric contours of copper in SOT show good definition, and the potential window for copper oxide formation (between peaks II and III) is wider (i.e., 0.15 V) than that for SOT (i.e., 0.12 V). On the other hand, the potential window for copper oxide electroreduction (between peaks IV and V), is narrower, 0.17 V, than that for SOT (i.e., 0.20 V).

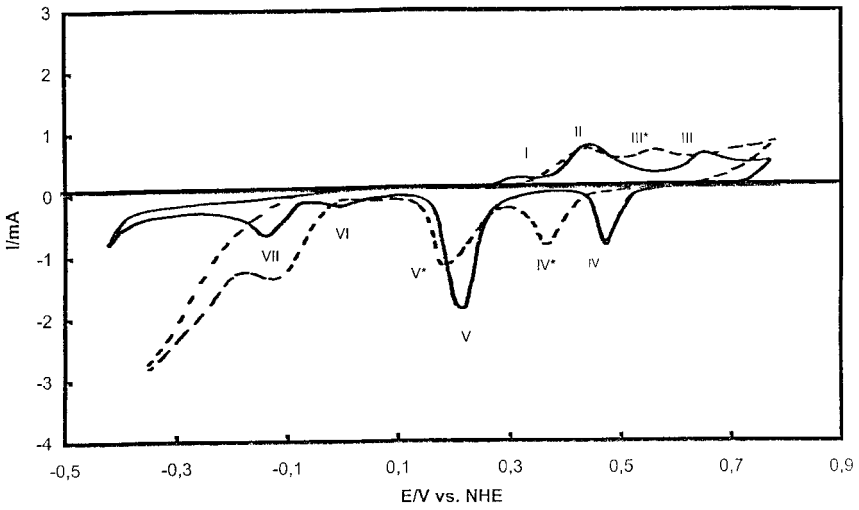

Fig. 5. Cyclic voltammogram of high-purity copper in aqueous 0.1 M NaOH (—) and SOT medium (----) run at $0.05\,V\,s^{-1}$ and 30 °C.

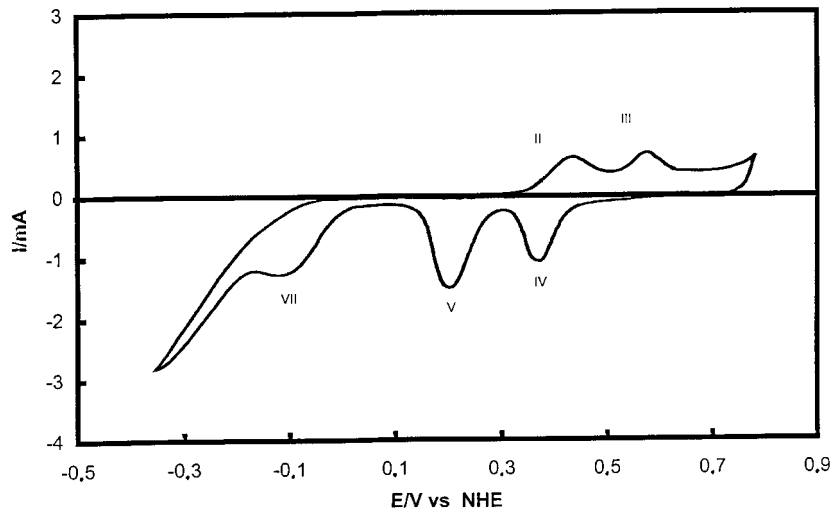

Fig. 6. Cyclic voltammogram of high-purity copper in deoxygenated carbonate–bicarbonate buffer solution run at $0.05\,V\,s^{-1}$ and 30 °C.

3.2. *Polarization curves*

Data obtained from steady state polarization curves were analysed as potential against log(current density) plots. E_{corr} and j_{corr} were calculated graphically [13, 14], from the intersection between the anodic (metal dissolution in oxygen-containing electrolytes and hydrogen evolution in oxygen-free solutions) and cathodic (oxygen electroreduction) branches of the semilogarithmic plots.

In this work, E_{corr} was distinguished from E_{rest}, the former being the potential obtained from the electrode kinetic experiments and the latter the open circuit value under any experimental condition.

3.2.1. Polarization curves for iron electrodes. Figures 7(a), (b) and (c) show the polarisation curves of commercially pure iron in SOT free of *S. platensis* saturated with air, nitrogen and oxygen, respectively. Different results were obtained when the iron probes were exposed to SOT solutions containing *S. platensis* at the fifth day of growth (C_1) with and without a light exposure (Figs 8(a) and (b), respectively). The analysis of the polarization curves for iron in the different media gave E_{corr} and j_{corr} (Table 3). It can be concluded that j_{corr} is mainly controlled by the concentration of dissolved oxygen. Moreover, the larger the oxygen concentration level, the higher the j_{corr} and the more positive E_{corr} [15, 16].

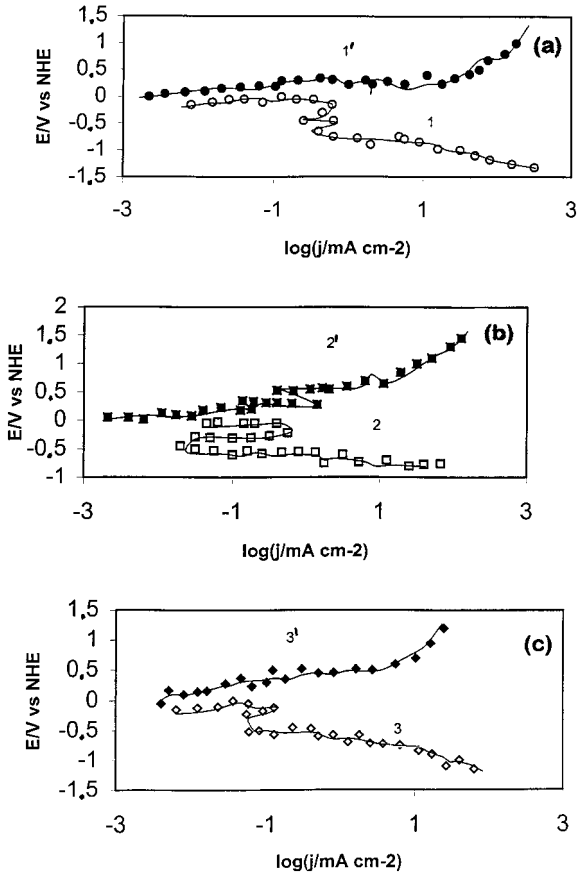

Fig. 7. Potentiostatic cathodic 1(○); 2(□); 3(◇) and anodic 1′(●); 2′(■); 3′(◆) polarization curves performed for iron in SOT medium: (a) air-saturated, (b) nitrogen-saturated, and (c) oxygen-saturated.

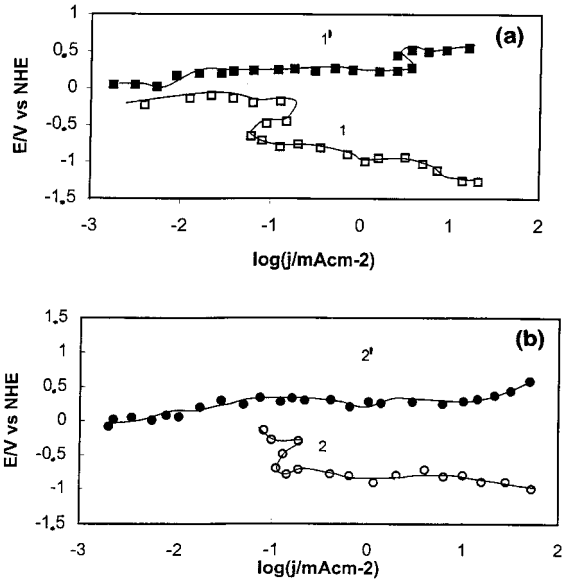

Fig. 8. Potentiostatic cathodic 1(□); 2(○) and anodic 1′(■); 2′(●) polarization curves performed for iron in SOT media containing *S. platensis* (C_1) saturated with air in different phases: (a) without light; (b) with light.

Polarization curves were also obtained with high-purity iron electrodes. In this case, E_{corr} was 50 mV more negative than that obtained with commercial probes, but almost the same j_{corr} (0.8 μA cm^{-2}) was obtained. In the presence of air and oxygen, j_{corr} increases to the same values of those obtained with commercially pure iron (70 and 85 μA cm^{-2}, respectively), and E_{corr} increases to −0.371 and −0.202 V, respectively. Constant $E_{corr} = -0.36$ V and $j_{corr} = 50$ and 20 μA cm^{-2} were obtained in SOT containing *S. platensis* at C_1 and C_2 in the dark. On the other hand, polarization curves run with iron in C_1 in the presence of light shows $j_{corr} = 100\ \mu$A cm^{-2} and $E_{corr} = -0.15$ V, that is, 50 mV more negative than that obtained with commercial probes.

3.2.2. Polarization curves for copper electrodes. Corrosion parameters of commercially pure copper are summarised in Table 4. In contrast to iron, E_{corr} for copper is independent of the presence or absence of the microalgae, that is $E_{corr} = 0.16$ V, coinciding

Table 3. Iron corrosion parameters, E_{corr} and j_{corr}, in different media at 30 °C

Fe probes	E_{corr} /V	j_{corr} /μA cm^{-2}
Nitrogen-saturated SOT	−0.373	1
Air-saturated SOT	−0.320	80
Oxygen-saturated SOT	−0.218	90
Air-saturated C_1 containing *S. platensis* in the dark	−0.237	40
Air-saturated C_2 containing *S. platensis* in the dark	−0.266	20
Air-saturated C_1 containing *S. platensis,* 5.4 kLux	−0.107	90

Table 4. Copper corrosion current density, j_{corr}, in different media at 30 °C

E_{corr} = 0.16 V (all cases)

Cu probes	j_{corr} /μA cm^{-2}
Nitrogen-saturated SOT	2
Air-saturated SOT	4
Oxygen-saturated SOT	5
Air-saturated C_1 containing *S. platensis* in the dark	7
Air-saturated C_2 containing *S. platensis* in the dark	4
Air-saturated C_1 containing *S. platensis*, 5.4 kLux	12

with the $Cu(OH)^+$/Cu standard potential value [17]. Therefore, an increase in the interfacial oxygen concentration would only produce higher values of j_{corr}, but no changes in E_{corr}. The bubbling of air in SOT produces a two-fold increase in j_{corr}, while in the presence of the microalgae (C_1, illuminated) j_{corr} increases six times. In all cases, the corrosion rate of copper is lower than that obtained with iron in the same solution.

For comparison, polarization curves for high-purity copper were obtained in the solutions tested above. The same electrochemical behaviour was observed between high-purity and commercially pure metals, that is, j_{corr} increased in the presence of interfacial oxygen (oxygen- and air-saturated solutions), and strongly increased in the presence of the microalgae (both in the dark and illuminated). Values of E_{corr} remained practically constant with a slightly more positive figure than that obtained with commercially pure metals, that is, 0.20 V.

3.3. *General comments*

The anodic branches of iron and copper polarization curves exhibit different trends. Constant values of E_{corr} in all solutions were found for copper, whereas increasing values for iron were observed, specially for dark and illuminated C_1 and C_2 culture media (Tables 3 and 4). This means that a direct determination of E_{rest} is insufficient to reach a conclusion about the corrosion properties of the metal. Therefore, a careful inspection of E_{corr} and j_{corr} has to be conducted to reach any conclusions about the metal stability.

It is known that the adhesion of microorganisms depends on the nature of the electrode, temperature and pH. Biofouling films are generally formed during microbial corrosion: so, in order to avoid them, polarization curves were conducted in SOT with immersion times as short as possible (< 1 h for each branch). In our case, the pH of SOT exceeds by almost one unit the optimum range for biofouling development, that is, 5–9 [18], so biofouling is not expected on both metals. The change in E_{rest} with time was tested as an indirect indication of the presence of biofilms. E_{rest} values for iron (Table 5) increase from nitrogen

Table 5. Iron and copper rest potentials in different media at 30 °C

Fe probes	E_{rest} /V
Nitrogen-saturated SOT	−0.35
Air-saturated SOT	−0.30
Oxygen-saturated SOT	−0.20
Air-saturated C_1 containing *S. platensis* in the dark	−0.17
Air-saturated C_2 containing *S. platensis* in the dark	−0.19
Air-saturated C_1 containing *S. platensis*, 5.4 kLux	−0.10
Cu probes	E_{rest} /V
Nitrogen-saturated SOT	0.18
Air-saturated SOT	0.19
Oxygen-saturated SOT	0.19
Air-saturated C_1 containing *S. platensis* in the dark	0.20
Air-saturated C_2 containing *S. platensis* in the dark	0.20
Air-saturated C_1 containing *S. platensis*, 5.4 kLux	0.20

to oxygen (or air) saturated solutions almost in the same way as in the case of E_{corr}, that is, there is no dramatic change in E_{rest} in the presence of the microalgae. In culture media containing *S. platensis*, there is no difference between the values of E_{rest} obtained for C_1 or C_2, but a big increase in E_{rest} for C_1 when the solution was illuminated. Thus, light influences the microbial corrosion; however, changes in E_{rest} with time (over 2 h) gave no significant variations. Careful visual inspection of iron at the end of the anodic branch of the polarization curve in SOT, showed that there was an organic film on the electrode (maybe a precursor of the biofilm) but no localised corrosion process was evident.

Moreover, Table 5 shows that the values of E_{rest} for copper are constant, as in the case of E_{corr}. In contrast to iron, visual inspection of the copper surface at the end of the anodic polarization curve in SOT showed no evidence of pitting or localised corrosion. No large cellular adherence or biofilm on copper was expected since its formation should have produced a large positive shift in E_{rest} (more than 0.10 V), a fact not observed in this work.

Metal corrosion in a microalgae-containing solution is controlled by the adherence of microorganisms to the electrode surface. Moreover, it is known that the possibility of microbial adherence on noble metals is smaller than on non noble electrodes [19], thus greater adherences of *S. platensis* are expected on iron, with higher j_{corr} values. Consequently, copper is the correct choice as metal-calefactor in cultivation baths. However, special care has to be taken in long-time assays, because of the high toxicity of copper ions for microalgae growth [19]. Further electrochemical analysis of these metals at larger exposure times have to be considered, together with the effect of biofouling, to reach conclusions about their industrial use.

4. Conclusions

The following remarks can now be made:

(i) The microalgae growth curves, that is, absorbance and oxygen concentration against cultivation time for *S. platensis*, are fingerprints of the oxygen biogeneration capability.
(ii) Cyclic voltammograms of copper and iron in carbonate–bicarbonate buffer exhibit similar profiles to those in SOT free of *S. platensis*.
(iii) The increase in dissolved oxygen concentration (with and without microalgae), produces a positive shift in the corrosion potential of iron. On the other hand, constant corrosion potentials for copper are found in air-saturated SOT (with and without the microalgae).
(iv) Short time measurements of E_{rest} are not suitable for predicting the corrosion properties of copper and iron in SOT containing *S. platensis*. No biofilms are observed on copper, but they are found on iron.
(v) Copper may be a correct choice for a metal calefactor with short cultivation times, since larger corrosion current densities are obtained for iron.

Acknowledgements

This work was financially supported by PEDECIBA (Programa de Desarrollo de Ciencias Básicas).

References

[1] A. Vonshak and A. Richmond, 'Mass Production of Spiruline. An Overview', *Biomass* (1988), pp. 233–43.
[2] A. Richmond, 'Spiruline Microalgae Biotechnology', (edited by Borowitska), (Cambridge University Press. Cambridge, UK, 1988).
[3] A. Richmond, 'CRC Handbook of Microalgae Mass Culture', (CRC Press, Boca Raton, FA, 1986).
[4] O. Ciferri, *Microbiol. Rev.* **47** (1983) 551.
[5] J. C. Weissman, R. P. Goebel and J. R. Benemann, *Biotechnol. & Bioeng.* **31** (1988) 336.
[6] M. Hirano, H. Mori, Y. Miura, N. Matunaga, M. Nakamura and T. Matsunaga, *Appl. Biochem. & Biotechnol.* **24/25** (1991) 183.
[7] S. C. Dexter, O. W. Siebert, D. J. Duquette and H. Videla, 'Use and Limitation of Electrochemical Techniques for Investigating Microbiological Corrosion', Corrosion, 89, Paper 616.
[8] S. M. Gerchakov, B. Little and P. Wagner, *Corrosion* **42** (1986) 689.
[9] ISO, 8407: 1991 (E) (UNIT).
[10] S. L. Marchiano, C. I. Elsner and A. J. Arvia, *J. Appl. Electrochem.* **10** (1980) 365.
[11] V. Brusic and T. J. Watson, 'Oxide and Oxide Films', (edited by J. W. Diggle) Vol. 1 (Marcel Dekker, New York, 1972).
[12] A. Wieckowski and E. Ghali, *Electrochim. Acta* **30** (1985) 1423.
[13] F. Mansfeld and B. Little, *Corros. Sci.* **32** (1991) 247.
[14] J. O' M. Bockris and D. M. Drazic, 'Electrochemical Science' (Taylor & Francis, London, 1972).
[15] R. S. Schebler-Guzmán, J. R. Vilche and A. J. Arvia, *Electrochim. Acta* **24** (1979) 395.
[16] B. R. Pearson and P. A. Brook, *Corros. Sci.* **32** (1991) 387.
[17] M. Pourbaix, 'Atlas of Electrochemical Equilibria' (Pergamon Press, Oxford, 1974), pp. 214–8.
[18] W. G. Characklis and K. E. Cooksey, *Adv. Appl. Microbiol.* **29** (1983) 93.
[19] G. Bitton and K. C. Marshall, 'Adsorption of Microorganisms to Surfaces' (J. Wiley & Sons, New York, 1980).